

Long-term effects of Na⁺/Ca²⁺ exchanger inhibition with ORM-11035 improves cardiac function and remodelling without lowering blood pressure in a model of heart failure with preserved ejection fraction

Uwe Primessnig^{1,2,3,4}, Taja Bracic², Jouko Levijoki⁵, Leena Otsomaa⁵,
Piero Pollesello⁵, Martin Falcke^{6,7}, Burkert Pieske^{1,3,4}, and Frank R. Heinzel^{1,3*}

¹Department of Internal Medicine and Cardiology, Charité – Universitätsmedizin Berlin, Campus Virchow-Klinikum, Berlin, Germany; ²Department of Cardiology, Medical University of Graz, Graz, Austria; ³DZHK (German Centre for Cardiovascular Research), Partner Site, Berlin, Germany; ⁴Berlin Institute of Health (BIH), Berlin, Germany; ⁵Critical Care, Orion Pharma, Espoo, Finland; ⁶Max Delbrück Center for Molecular Medicine, Berlin, Germany; and ⁷Department of Physics, Humboldt Universität, Berlin, Germany

Received 9 January 2019; revised 26 August 2019; accepted 2 September 2019; online publish-ahead-of-print 24 November 2019

Aims

Heart failure with preserved ejection fraction (HFpEF) is increasingly common but there is currently no established pharmacological therapy. We hypothesized that ORM-11035, a novel specific Na⁺/Ca²⁺ exchanger (NCX) inhibitor, improves cardiac function and remodelling independent of effects on arterial blood pressure in a model of cardiorenal HFpEF.

Methods and results

Rats were subjected to subtotal nephrectomy (NXT) or sham operation. Eight weeks after intervention, treatment for 16 weeks with ORM-11035 (1 mg/kg body weight) or vehicle was initiated. At 24 weeks, blood pressure measurements, echocardiography and pressure–volume loops were performed. Contractile function, Ca²⁺ transients and NCX-mediated Ca²⁺ extrusion were measured in isolated ventricular cardiomyocytes. NXT rats (untreated) showed a HFpEF phenotype with left ventricular (LV) hypertrophy, LV end-diastolic pressure (LVEDP) elevation, increased brain natriuretic peptide (BNP) levels, preserved ejection fraction and pulmonary congestion. In cardiomyocytes from untreated NXT rats, early relaxation was prolonged and NCX-mediated Ca²⁺ extrusion was decreased. Chronic treatment with ORM-11035 significantly reduced LV hypertrophy and cardiac remodelling without lowering systolic blood pressure. LVEDP [14 ± 3 vs. 9 ± 2 mmHg; NXT ($n = 12$) vs. NXT + ORM ($n = 12$); $P = 0.0002$] and BNP levels [71 ± 12 vs. 49 ± 11 pg/mL; NXT ($n = 12$) vs. NXT + ORM ($n = 12$); $P < 0.0001$] were reduced after ORM treatment. LV cardiomyocytes from ORM-treated rats showed improved active relaxation and diastolic cytosolic Ca²⁺ decay as well as restored NCX-mediated Ca²⁺ removal, indicating NCX modulation with ORM-11035 as a promising target in the treatment of HFpEF.

Conclusion

Chronic inhibition of NCX with ORM-11035 significantly attenuated cardiac remodelling and diastolic dysfunction without lowering systemic blood pressure in this model of HFpEF. Therefore, long-term treatment with selective NCX inhibitors such as ORM-11035 should be evaluated further in the treatment of heart failure.

Keywords

Na⁺/Ca²⁺ exchanger • ORM-11035 • Heart failure with preserved ejection fraction • Cardiomyocyte • Calcium

*Corresponding author. Department of Cardiology, Charité-University Medicine Berlin, Campus Virchow-Klinikum, Augustenburger Platz 1, 13353 Berlin, Germany. Tel: +49 30 450553702, Fax: +49 30 4507553702, Email: frank.heinzel@charite.de

Introduction

Heart failure (HF) is increasingly common in the general population implicating a considerable socioeconomic burden. A large number of patients with signs and symptoms of HF present with structurally remodelled hearts but a preserved ejection fraction (HFpEF). HFpEF is regarded as a heterogeneous clinical syndrome with different aetiologies.¹ Common clinical risk factors for HFpEF include arterial hypertension, diabetes and renal failure. Currently, no pharmacological therapy has been proven effective in improving prognosis in HFpEF patients. Recently, we have reported a cardiorenal model of HFpEF in rats, which mimics many of the features that define the clinical HFpEF syndrome.² Parameters of HF *in vivo* correlated with impaired relaxation of cardiomyocytes and slowed decay of the intracellular Ca^{2+} transient. In this model, chronic inhibition of the $\text{Na}^+/\text{Ca}^{2+}$ exchanger (NCX) with SEA0400 improved diastolic function and cardiac remodelling *in vitro* and *in vivo*, suggesting a role of increased reverse-mode NCX activity (Ca^{2+} import). However, while treatment with SEA0400 improved relaxation, it was associated with a reduction in systemic blood pressure, likely related to SEA0400 inhibitory effects on L-type Ca^{2+} channels.² In the present study, we employed a novel NCX inhibitor, ORM-11035, to investigate whether a more specific NCX inhibition confirms the role of the NCX in this model of HFpEF and may improve cardiac function and remodelling without lowering systemic blood pressure.

Methods

All experiments were approved by the local Ethics Committee (GZ: BMWF-66.010/0040-II/3b/2012) and performed in agreement with the Guidelines for the Care and Use of Laboratory Animals (National Institutes of Health, USA). Animals were housed in a 12 h light/dark regime under conventional conditions in the local animal facility with free access to food and water. Experiments were performed as previously described.² Forty young male 8-week old Wistar rats (HsdRC-CHan, Harlan, Italy) with a body weight between 250 and 275 g underwent subtotal (5/6) nephrectomy (NXT) or sham operation (Sham) in a one-time intervention.³ Animals were observed for 24 weeks post-operatively. Non-invasive blood pressure measurements were performed weekly (tail-cuff method). Treatment with ORM-11035 (1 mg/kg body weight/day divided into two daily doses) or vehicle via oral gavage was performed starting 8 weeks post-surgery for 16 weeks including the day of final experiment. At 24 weeks transthoracic echocardiography was performed in anaesthetized rats with heart rate continuously measured by electrocardiographic electrodes. Measurements were performed to assess changes in cardiac function and dimensions from at least three consecutive cardiac cycles under stable conditions using standard formulas. Invasive haemodynamic measurements (pressure–volume loops) were performed as previously described. The pressure–volume conductance catheter (SPR-838, Millar Instruments, Houston, TX, USA) was inserted into the right carotid artery and advanced into the ascending aorta and then into the left ventricle. Parameters of systolic and diastolic function including left ventricular (LV) end-systolic pressure, LV end-diastolic pressure (LVEDP), LV end-systolic volume, LV end-diastolic volume, stroke volume, cardiac output, LV ejection fraction, maximal slope of LV systolic pressure increment (dP/dt_{max}), maximal slope of diastolic pressure decrement

(dP/dt_{min}) and isovolumetric relaxation constant Tau (IVRc Tau) were measured and calculated according to standard formulas. Following the invasive measurements, animals were sacrificed and organ morphology as well as isolation of LV cardiomyocytes were performed. Additionally, blood and urine samples were collected for the analysis of brain natriuretic peptide (BNP) levels, serum creatinine, serum urea, glomerular filtration rate and proteinuria.

ORM-11035 efficacy and selectivity

The CAS code for ORM-11035 is 786642-16-8, with chemical name butanamide, 2-amino-N-[6-[(3,4-dihydro-2-phenyl-2H-1-benzopyran-6-yl)oxy]-3-pyridinyl]-3-methyl-,(2R). The patent number is WO 2003/006452. The concentration–response relationship for ORM-11035 on NCX was measured in Sf9 cells stably transfected with human 1.1 NCX by measuring reverse-mode NCX Ca^{2+} influx with Ca^{2+} indicator Fluo-4. The hERG current concentration response for ORM-11035 was quantified in HEK293 cells by patch-clamping. The L-type Ca^{2+} current concentration response for ORM-11035 was quantified in IMR-32 human neuroblastoma cells measuring Ca^{2+} influx by fluorescent Ca^{2+} indicator (Fluo-4). All experiments were performed at 37°C. The fluorescence value, maximum minus baseline, was calculated for each well with ScreenWorks 2.0 software. Dose–response curves for the ORM compounds were constructed from typically a mean of seven separate wells at each of five different concentrations on a plate. Results are expressed as mean \pm standard deviation for number of plates (online supplementary *Methods S1*).

Cardiomyocyte measurements in the heart failure with preserved ejection fraction model

Cardiomyocytes from NXT and Sham rats were isolated from the same animals that underwent *in vivo* characterization following enzymatic digestion of the explanted Langendorff-perfused heart as previously described.² LV cardiomyocytes were loaded with the Ca^{2+} indicator Fluo-4 AM (Molecular Probes, Leiden, The Netherlands) and transferred to a confocal line scanning microscope (LSM 510 Meta, Zeiss, Germany). In a subset of cardiomyocytes (only Sham, NXT and NXT + ORM-11035), LV cardiomyocytes were loaded with Fura-2AM (1 $\mu\text{mol/L}$) for $[\text{Ca}^{2+}]_i$ measurements (excitation at 340/380 nm, emission >510 nm, background corrected) and transferred to a ratiometric fluorescence microscope setup (Horiba PTI, Tokyo, Japan, on Zeiss Axiovert microscope, Jena, Germany) additionally equipped with a charge-coupled device camera for edge detection (cell shortening). Cardiomyocytes were continuously superfused with superfusion solution and stimulated in an electrical field at both setups without additional application of ORM-11035 during *in vitro* experiments. Ca^{2+} -transient (CaT) amplitude (F, normalized to diastole, F0) and time to half-maximal decay (CaT RT50) were calculated from confocal line scan images (1.56 ms/line along the longitudinal axis of the cell and analysed using custom made algorithms coded in IDL).^{4,5} Late diastolic $[\text{Ca}^{2+}]_i$ (average of 30 ms before stimulus) was quantified ratiometrically, and cell shortening amplitude (percent of resting length) and kinetics (time to 50% relaxation, CS RT50) were calculated. All measurements were performed at 1 Hz steady state (>30 s). For the assessment of sarcoplasmic reticulum (SR) and NCX Ca^{2+} transport in intact cardiomyocytes a superfusion solution with 30 mmol/L caffeine for 10 s was applied

via a rapid perfusion line (<1 s wash-in) in Fura-2AM-loaded cardiomyocytes following 1 Hz steady state stimulation. SR Ca^{2+} content was quantified as the amplitude of the caffeine-induced Ca^{2+} transient. Time constant of Ca^{2+} decay in the presence of caffeine (TAU_{caff} , mono-exponential fit) was quantified as a measure of NCX forward mode activity. SR Ca^{2+} -ATPase (SERCA)-related time constant of Ca^{2+} decay at 1 Hz ($\text{TAU}_{\text{SERCA}}$) was calculated from TAU_{caff} and tau of the last stimulated CaT (TAU_{stim}), by the formula: $\text{TAU}_{\text{SERCA}} = 1/(1/\text{TAU}_{\text{stim}} - 1/\text{TAU}_{\text{caff}})$. Fractional contribution of not SERCA-related CaT decay to TAU_{stim} was calculated as $(1/\text{TAU}_{\text{caff}})/(1/\text{TAU}_{\text{stim}})$.

Reporting according to the ARRIVE guidelines

No animals died during the procedure. With an empiric goal of 15–20 cardiomyocytes per group, we chose 4–6 animals per group for isolation of cardiomyocytes. All animals included for cellular measurements provided at least three cells for analysis. The decision to isolate cardiomyocytes from an animal was made before the start of the final experiment (*in vivo* measurements). Cardiomyocytes that did not complete the full protocol [e.g. 1 Hz stimulation at steady state + caffeine response with rapid (<1 s time to monophasic peak of Ca^{2+} release)] or did not follow each stimulus were completely excluded from the analysis.

Modelling

In order to model NCX current at different $[\text{Na}]_i$ during the cardiac cycle, we used the mathematical model for rabbit myocyte electrophysiology and Ca^{2+} dynamics developed by Mahajan *et al.*^{6,7}

Statistics

Analyses were done using two-way ANOVAs (Figures 1–4; online supplementary Figure S1 and Tables S1–S3) or two-way repeated measures ANOVA (online supplementary Figure S2) followed by pairwise comparisons with Bonferroni–Holm correction. One-way ANOVA with Tukey post-hoc test was used on the subset of ratiometric data (Figure 5; online supplementary Table S4). An alpha level (*P*) of 5% was used for all tests. Data were analysed using GraphPad Prism (GraphPad Software, Inc., La Jolla, CA, USA). Values are given as mean \pm standard deviation. Error bars denote standard deviation.

An expanded Material and Methods section is available in the online supplementary Methods S1.

Results

ORM-11035 selectivity and bioavailability

ORM-11035 concentration–effect curves *in vitro* yielded an IC_{50} of 150 nmol/L for NCX (online supplementary Figure S3), 5 $\mu\text{mol/L}$ for the L-type Ca^{2+} channel and 1.1 $\mu\text{mol/L}$ for hERG.

Heart failure with preserved ejection fraction phenotype after subtotal nephrectomy in rats

Following subtotal NXT, rats showed cardiac remodelling, e.g. LV hypertrophy [LV mass: 1944 ± 146 vs. 2581 ± 208 mg; Sham

($n = 8$) vs. NXT ($n = 12$); $P < 0.0001$], left atrial enlargement and diastolic dysfunction with LVEDP elevation [6 ± 2 vs. 14 ± 3 mmHg; Sham ($n = 8$) vs. NXT ($n = 12$); $P < 0.0001$], increased E/e' ratio [19 ± 2 vs. 31 ± 3 ; Sham ($n = 8$) vs. NXT ($n = 12$); $P < 0.0001$] as well as preserved ejection fraction, congestion and increased BNP levels (Figures 1, 2 and online supplementary Tables S1, S2). Moreover, in cardiomyocytes from untreated NXT rats, early relaxation was prolonged (Figure 4A, 4E) and NCX-mediated Ca^{2+} extrusion was decreased (Figure 5A, 5D) suggesting increased NCX reverse-mode activity during relaxation in these HFpEF rats.

Effects of chronic treatment with ORM-11035 on heart failure with preserved ejection fraction phenotype *in vivo*

NXT rats showed typical signs and symptoms of HFpEF as previously reported by Primessnig *et al.*² This HFpEF-like phenotype was present at 8 weeks following subtotal NXT. ORM-11035 treatment with 1 mg/kg/day was started at week 8 after NXT/Sham operation and was applied for 16 weeks (online supplementary Figure S4). Long-term chronic treatment with the novel compound ORM-11035 reversed cardiac remodelling and diastolic dysfunction in these HFpEF rats (online supplementary Tables S1 and S2). Heart weight/body weight ratio [3.24 ± 0.3 vs. 2.81 ± 0.3 mg/g; NXT ($n = 12$) vs. NXT + ORM ($n = 12$); $P = 0.004$], lung weight/body weight ratio [4.48 ± 0.56 vs. 3.85 ± 0.49 mg/g; NXT ($n = 12$) vs. NXT + ORM ($n = 12$); $P = 0.02$], LV mass, LV relative wall thickness, and left atrial size [29 ± 3 vs. 25 ± 3 mm²; NXT ($n = 12$) vs. NXT + ORM ($n = 12$); $P = 0.003$] were significantly reduced after treatment with ORM-11035 (Figure 1A–F). Treatment with ORM-11035 had no effect on systolic blood pressure [156 ± 3 vs. 153 ± 5 mmHg; NXT ($n = 12$) vs. NXT + ORM ($n = 12$); $P = \text{ns}$] or diastolic blood pressure, measured by weekly non-invasive blood pressure measurements (online supplementary Figure S2) or invasively at 24 weeks during final experiments (Figure 1G and 1H; online supplementary Table S1). Diastolic dysfunction reflected by LVEDP [14 ± 3 vs. 9 ± 2 mmHg; NXT ($n = 12$) vs. NXT + ORM ($n = 12$); $P = 0.0002$], IVRc Tau [9.5 ± 0.6 vs. 8.7 ± 0.8 ms; NXT ($n = 12$) vs. NXT + ORM ($n = 12$); $P = 0.006$] as well as E/e' [31 ± 3 vs. 24 ± 2 ; NXT ($n = 12$) vs. NXT + ORM ($n = 12$); $P < 0.0001$] and BNP levels [71 ± 12 vs. 49 ± 11 pg/mL; NXT ($n = 12$) vs. NXT + ORM ($n = 12$); $P < 0.0001$] were significantly reduced after chronic treatment with ORM-11035 in NXT (Figures 2A, 2B, 2E, 3A–C) while LV ejection fraction and heart rate (Figure 2C and 2D) were unchanged.

Improved renal function after long-term treatment with ORM-11035

Renal function was significantly improved in NXT rats after treatment with ORM-11035 for 16 weeks. Serum creatinine [78.56 ± 12.87 vs. 55.96 ± 8.27 $\mu\text{mol/L}$; NXT ($n = 12$)

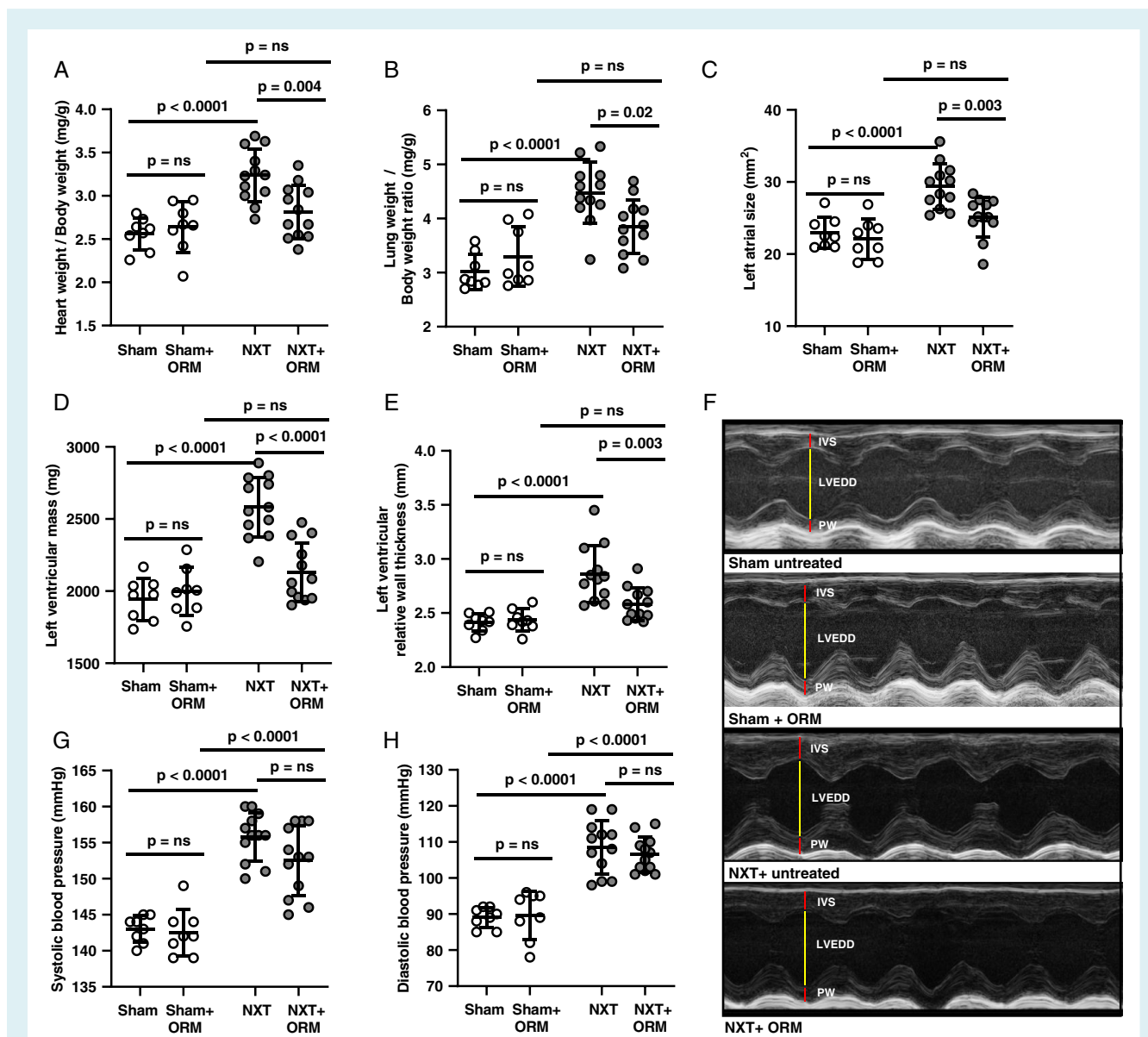


Figure 1 Effects of long-term chronic treatment with ORM-11035 on cardiac remodelling and systemic blood pressure in heart failure with preserved ejection fraction rats. (A) Heart weight/body weight ratio, (B) lung weight/body weight ratio, (C) left atrial size, (D) left ventricular mass, and (E) left ventricular relative wall thickness are significantly reduced in nephrectomy (NXT) + ORM-treated animals compared to untreated NXT rats. (F) Echocardiographic M-mode images of the left ventricle in Sham and NXT-treated or untreated with ORM. (G) Systolic blood pressure and (H) diastolic blood pressure are not affected after ORM treatment in Sham and NXT animals. Symbols = animals. Data are mean \pm standard deviation. Analysis using two-way ANOVA. Groups are Sham ($n = 8$), Sham + ORM ($n = 8$), NXT ($n = 12$) and NXT + ORM ($n = 12$). IVS, interventricular septum; LVEDD, left ventricular end-diastolic diameter; PW, posterior wall.

vs. NXT + ORM ($n = 12$; $P < 0.001$) and serum urea were significantly reduced while glomerular filtration rate (19 ± 2 vs. 24 ± 3 mL/min; NXT ($n = 12$) vs. NXT + ORM ($n = 12$); $P < 0.0001$) significantly improved after long-term admission of ORM-11035. Additionally, serum sodium, potassium, and proteinuria [3.16 ± 1 vs. 2.01 ± 0.7 g/L; NXT ($n = 12$) vs. NXT + ORM ($n = 12$); $P = 0.009$] were reduced in NXT rats treated with ORM-11035 (online supplementary Table S1).

ORM-11035 improves cardiomyocyte relaxation and cytosolic Ca^{2+} decay

Left ventricular cardiomyocyte cell shortening amplitude tended to be lower in NXT vs. Sham animals (Figure 4A and 4C; online supplementary Table S3). ORM-11035 did not significantly alter contraction amplitude in Sham or NXT (Figure 4A and 4C; online supplementary Table S3). ORM-11035 significantly accelerated relaxation time (CS RT50) in NXT [73.1 ± 24.8 vs. 47.5 ± 14.2 ms;

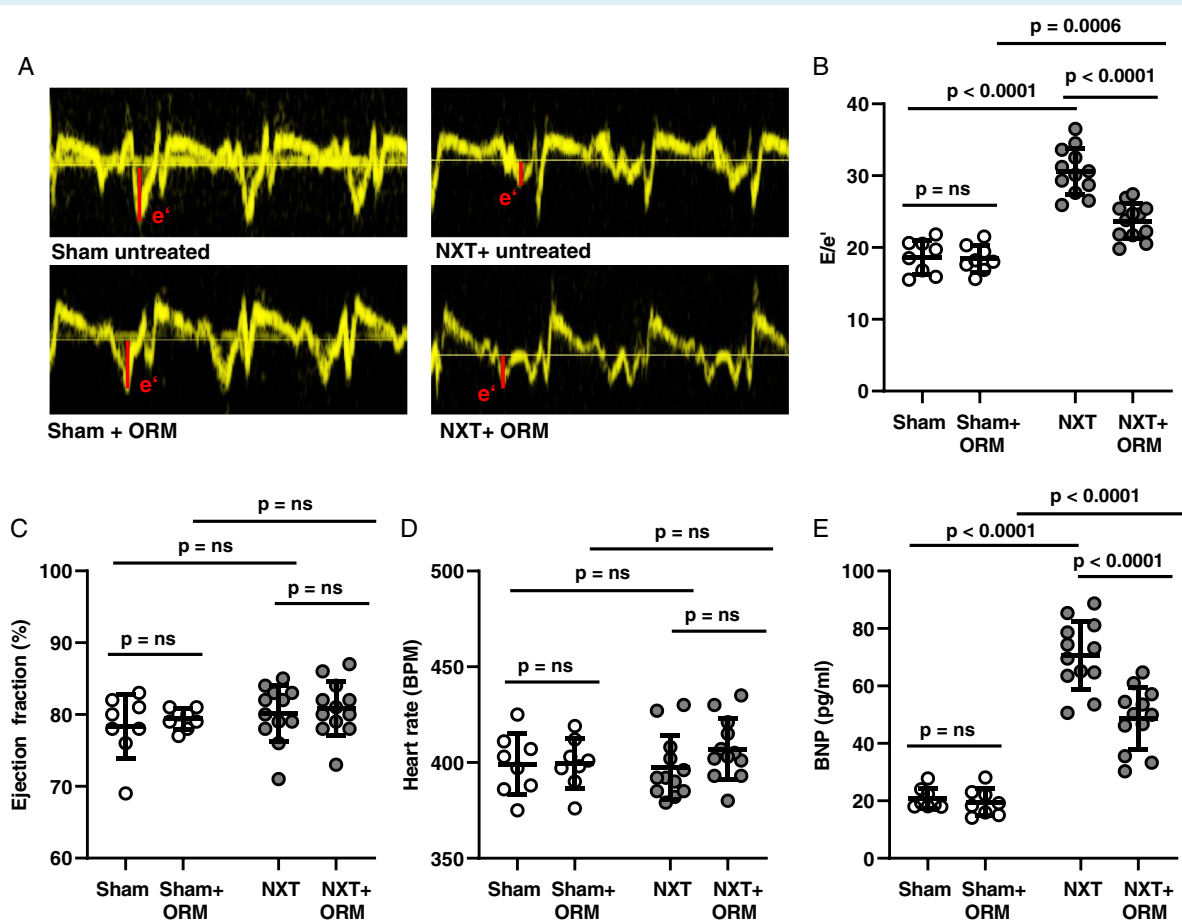


Figure 2 Chronic treatment with ORM-11035 reduces E/e' and brain natriuretic peptide (BNP) levels while heart rate and left ventricular ejection fraction are unchanged in heart failure with preserved ejection fraction (HFpEF) rats. (A) Examples of tissue Doppler measured e' in Sham and nephrectomy (NXT) animals treated or untreated with ORM. (B) Echocardiographic measured E/e' shows a significant reduction after ORM treatment in HFpEF rats. (C) Left ventricular ejection fraction and (D) heart rate are unchanged after ORM admission in Sham and NXT rats. (E) BNP levels are significantly reduced in NXT + ORM-treated HFpEF rats compared to untreated animals. Symbols = animals. Data are mean \pm standard deviation. Analysis using two-way ANOVA. Groups are Sham ($n = 8$), Sham + ORM ($n = 8$), NXT ($n = 12$) and NXT + ORM ($n = 12$).

NXT ($n = 22$) vs. NXT + ORM ($n = 15$); $P = 0.0003$] (Figure 4A and 4E; online supplementary Table S3). More rapid cell re-lengthening *in vitro* correlated with reduced LVEDP in the same animals *in vivo* (Figure 3D). In analogy to cell shortening amplitude, the amplitude of LV cardiomyocyte Ca^{2+} transients were slightly but significantly decreased in NXT vs. Sham rats, while no significant difference was observed in ORM-11035-treated vs. untreated NXT animals (Figure 4B and 4D; online supplementary Table S3). Ca^{2+} removal from the cytosol (CaT RT50) was slowed in NXT vs. Sham. ORM-11035 had no effect on cytosolic Ca^{2+} removal in Sham but significantly accelerated prolonged Ca^{2+} removal in NXT [CaT RT50: 171.8 ± 36 vs. 130.6 ± 32.5 ms; NXT ($n = 16$) vs. NXT + ORM ($n = 18$); $P = 0.002$] (Figure 4B and 4F; online supplementary Table S3). Concurrent, TAU of the CaT was prolonged in NXT vs. Sham and significantly ameliorated in ORM-11035-treated NXT animals (Figure 4F; online supplementary Table S3). Radiometric measurements revealed unchanged end-diastolic

$[Ca^{2+}]_i$ (Figure 5B). SR calcium content was decreased in NXT vs. Sham animals but was not affected by ORM treatment (Figure 5C; online supplementary Table S4). During caffeine application, cytosolic Ca^{2+} removal attributed to NCX (forward mode) was significantly slower in NXT vs. Sham. Chronic ORM-11035 treatment significantly ameliorated the slowed non-SERCA-dependent cardiomyocyte Ca^{2+} extrusion in NXT (Figure 5A and 5D; online supplementary Table S4). The SERCA-related cytosolic Ca^{2+} decay constant during electrical stimulation (TAU_{SERCA}), as calculated from TAU_{stim} and $TAU_{caffeine}$, was prolonged in NXT and restored in NXT + ORM (Figure 5F). In addition, the calculated contribution of not SERCA-related decay to the electrically stimulated Ca^{2+} transient was reduced in NXT vs. Sham (Figure 5G) with variable but non-significant change in NXT + ORM. In summary, LV cardiomyocytes from chronically ORM-treated rats showed improved active relaxation and diastolic cytosolic Ca^{2+} decay as well as restored NCX-mediated Ca^{2+} removal.

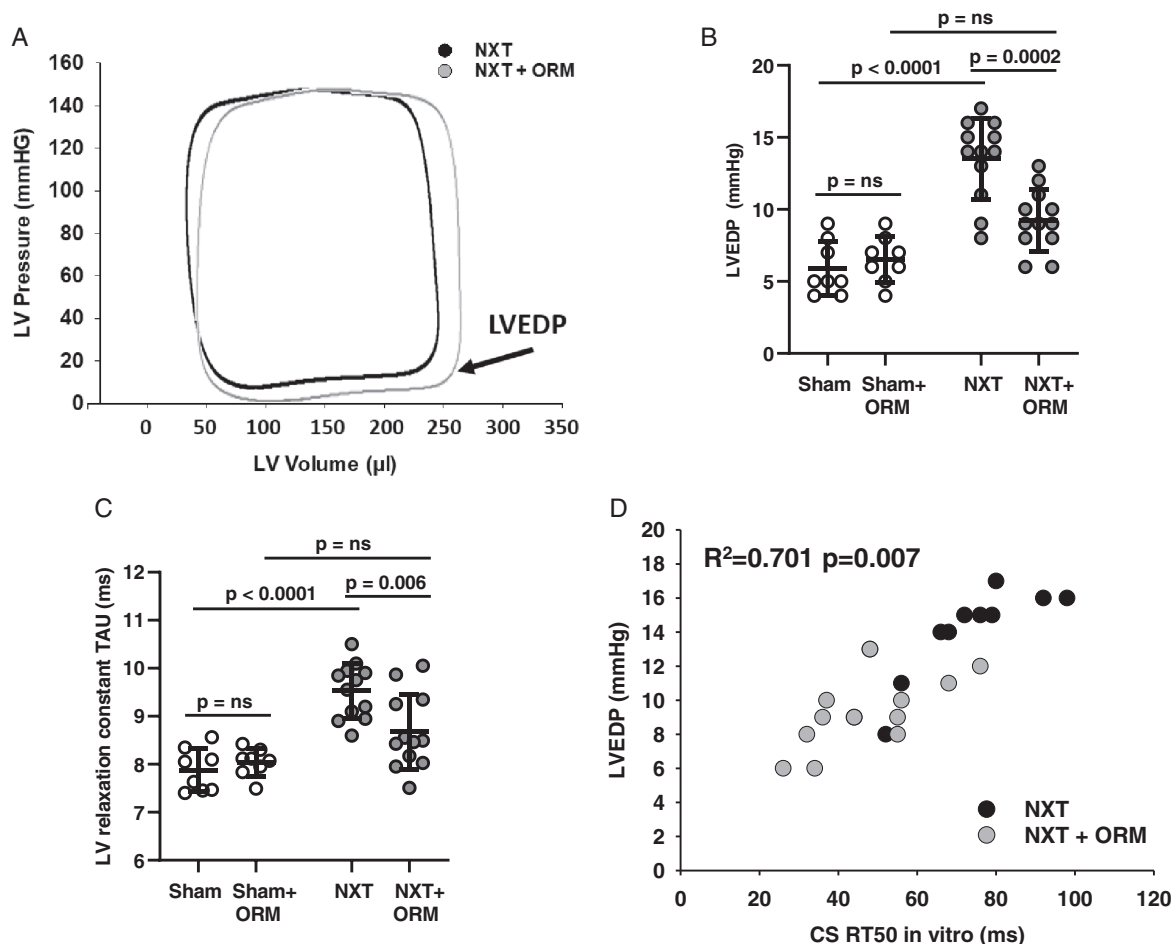


Figure 3 ORM-11035 attenuates diastolic dysfunction in heart failure with preserved ejection fraction rats. (A) Example pressure–volume loop recordings from nephrectomy (NXT) + ORM (gray) and NXT untreated (black) animals. (B) Chronic treatment with ORM for 16 weeks attenuates (B) left ventricular end-diastolic pressure (LVEDP) and (C) left ventricular (LV) relaxation constant TAU. Symbols = animals. Data are mean \pm S.D. *P* – values. Analysis using two-way ANOVA. Groups are Sham (*n* = 8), Sham + ORM (*n* = 8), NXT (*n* = 12) and NXT + ORM (*n* = 12). (D) Rapid cell re-lengthening (CS RT50) *in vitro* correlated with reduced LVEDP in the same animals *in vivo* (NXT and NXT + ORM). Symbol = cell average/heart.

Role of altered $\text{Na}^+/\text{Ca}^{2+}$ exchanger and SERCA activity and increased $[\text{Na}^+]_i$ for cytosolic Ca^{2+} decay in a mathematical cell model

We explored the effects of altered NCX and SERCA activity on cytosolic Ca^{2+} and Na^+ in a mathematical rabbit myocyte model. As shown in the online supplementary Figure S1A, a reduction of SERCA activity to 75% of control and increased NCX activity lead to a slowed Ca^{2+} transient decay mimicking the changes observed in the present HFpEF model. Increased NCX activity leads to a small increase in cytosolic $[\text{Na}^+]_i$ (online supplementary Figure S1B). In another simulation (online supplementary Figure S1C) we assumed a stronger elevated $[\text{Na}^+]_i$, which then induces reduced overall NCX forward mode activity (lower integral) and a leftward shift of the peak forward mode

activity. Ca^{2+} transients in NXT combining increased $[\text{Na}^+]_i$ (20 vs. 14 mM in control), increased NCX activity (>50% of control) and reduced SERCA (80% of control). Inhibition of NCX and restoration of SERCA activity with ORM improves diastolic Ca^{2+} decay. (Figure 3D)

Discussion

In the present study, chronic treatment with the novel NCX inhibitor ORM-11035 was effective in ameliorating signs and symptoms in a rat model of manifest cardiorenal HFpEF. In addition, we demonstrate that the beneficial effects of this specific NCX inhibitor on myocardial function and remodelling are independent of the blood pressure-lowering effect previously observed *in vivo* with SEA0400,² which implies that treatment of HF *in vivo* involves improvement of intrinsic cardiomyocyte function.

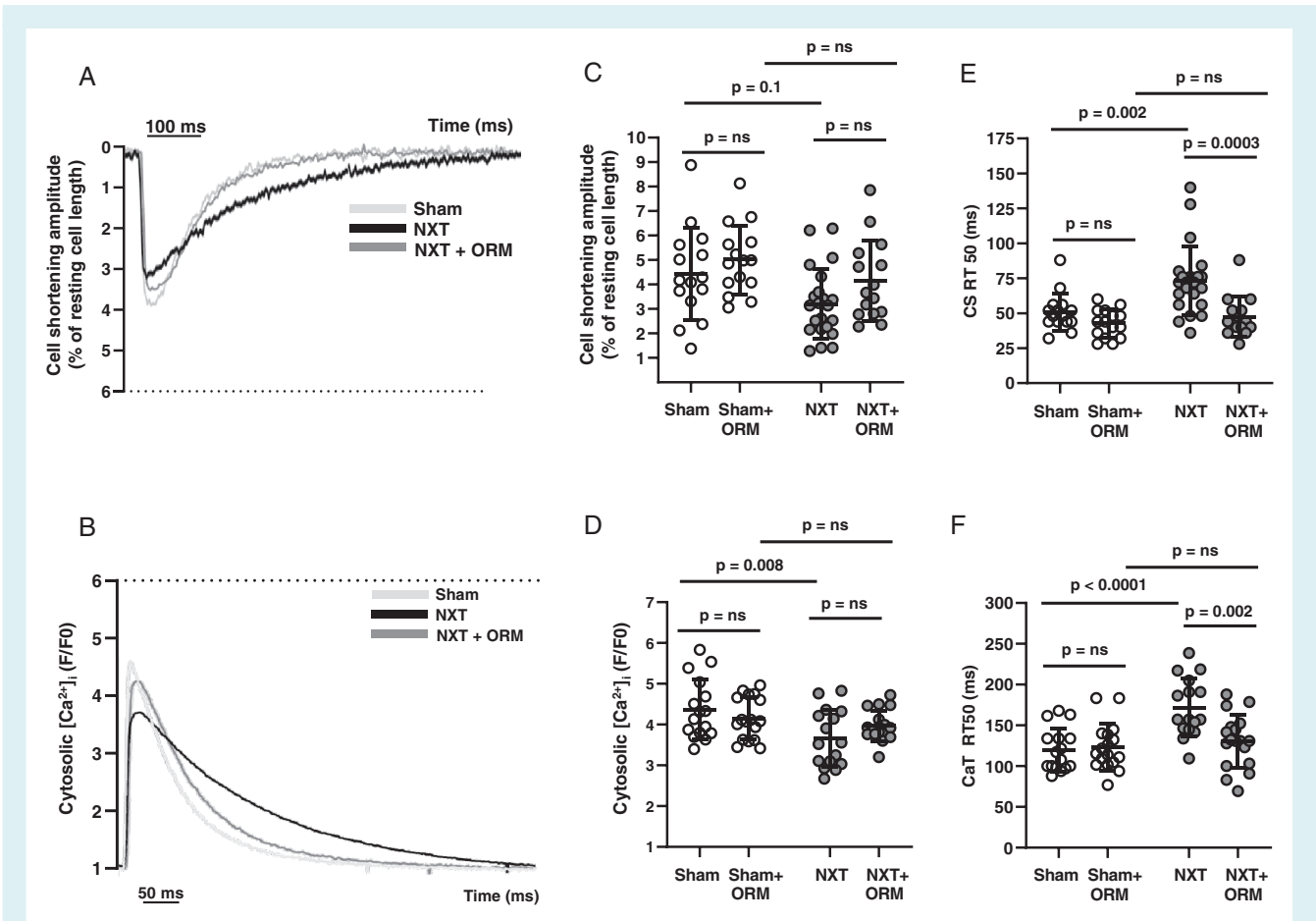
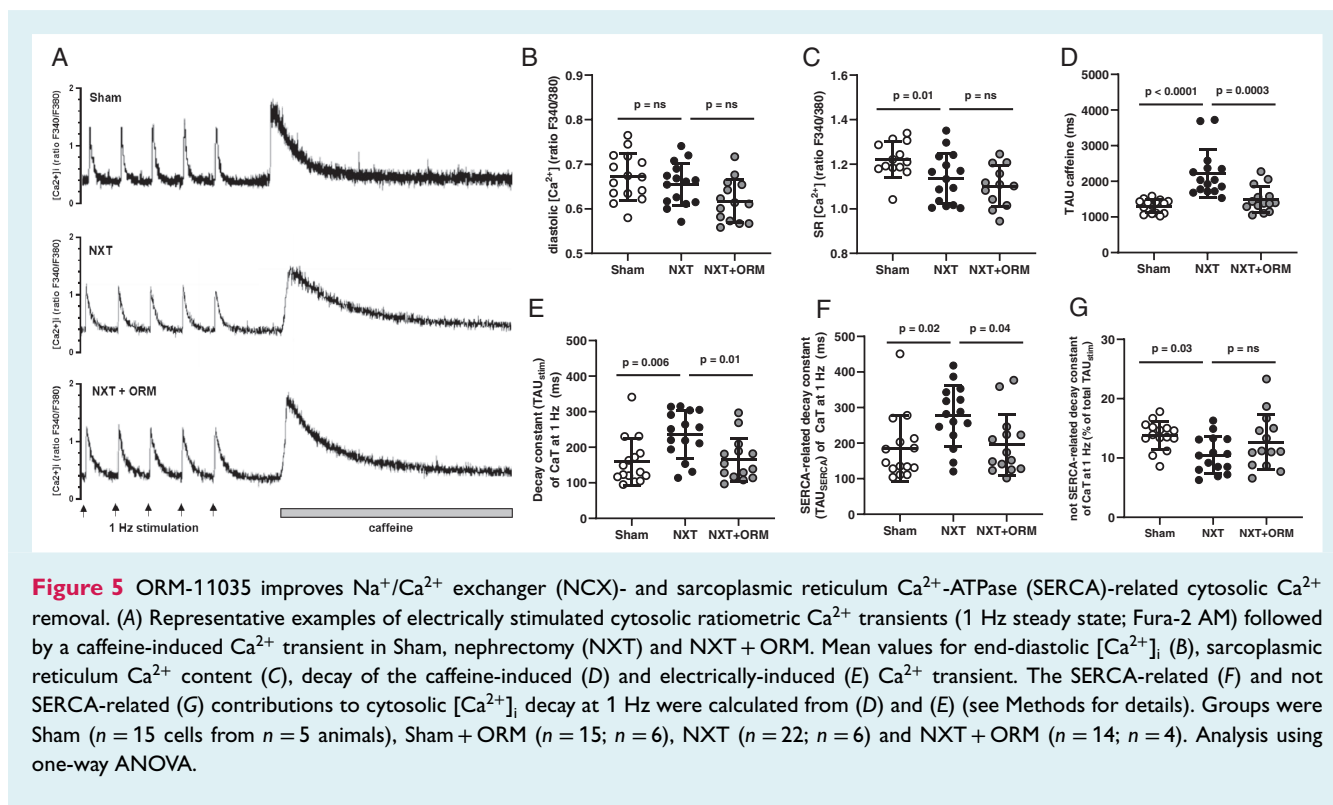


Figure 4 ORM-11035 accelerates contraction and cytosolic Ca^{2+} decay in left ventricular cardiomyocytes from nephrectomy (NXT)-treated rats. Representative example of cell shortening (A) and cytosolic Ca^{2+} transients (B; confocal; Fluo-4 AM) at 1 Hz in cardiomyocytes from Sham, NXT and NXT + ORM. Left ventricular cardiomyocyte cell shortening amplitude tended to be lower and Ca^{2+} transient (CaT) amplitude was lower in NXT vs. Sham-treated animals (C, D). Contraction and CaT amplitudes in Sham as well as in NXT were not affected by ORM. (B) Time to half-maximal cardiomyocyte relaxation (CS RT50) and time to half-maximal cytosolic CaT decay were significantly prolonged in NXT vs. Sham (E, F). ORM significantly accelerates relaxation time (CS RT50) and CaT decay in NXT. Symbols = individual cardiomyocytes. Groups were Sham ($n = 15$ cells from $n = 4$ animals), Sham + ORM ($n = 15$; $n = 5$), NXT ($n = 22$; $n = 6$) and NXT + ORM ($n = 15$; $n = 4$). Analysis using two-way ANOVA.

HFpEF is an increasingly commonly diagnosed clinical manifestation of various systemic disease entities resulting in cardiac involvement with diastolic dysfunction.¹ Chronic kidney disease with moderately to severely impaired renal function is observed in almost half of HFpEF patients and renal dysfunction may be pivotal in an even larger fraction of patients with HFpEF.^{8,9} Management of HFpEF is currently limited to symptomatic therapy of congestion using diuretics and treatment of associated co-morbidities. Targeting classical pathways over-activated in HF with reduced ejection fraction (HFrEF) such as the renin-angiotensin system or beta-blockade generally have not been effective.¹⁰ It has been proposed that the cellular mechanisms underlying HFrEF (with progressive loss of cardiomyocytes) are fundamentally different from HFpEF, where inflammation and endothelial dysfunction trigger cardiomyocyte dysfunction, mainly due to increased passive stiffness.¹¹ Previously, we and others have shown that active, i.e.

Ca^{2+} -dependent, cardiomyocyte relaxation contributes to diastolic dysfunction in HFpEF.^{2,12} Cytosolic Ca^{2+} decay in physiological conditions is mediated mainly by SERCA-dependent Ca^{2+} reuptake into the SR and to a lesser extent by the sarcolemmal NCX. NCX works in forward (Ca^{2+} out, Na^{+} in) or reverse mode depending on local (subsarcolemmal) ion concentrations and NCX regulation, and several changes in direction during the normal action potential may occur.¹³ Several mechanisms may be involved in alteration of NCX-dependent cytosolic Ca^{2+} removal in this HFpEF model. The cellular phenotype is characterized by a slowed diastolic Ca^{2+} decay without signs of cellular Ca^{2+} overload, as in NXT diastolic Ca^{2+} is unchanged and SR Ca^{2+} content is decreased. NCX protein expression is increased,² suggesting increased NCX activity. Slowed cytosolic Ca^{2+} decay can be explained by reduced SERCA activity (Figure 5F; online supplementary Figure S1A), but may also involve increased NCX activity in reverse mode during the phase



of relaxation, as observed with increased intracellular $[\text{Na}]_i$ and contributing to diastolic dysfunction in HFpEF.^{14,15} While limited by species differences (rabbit vs. rat), our simulations in a mathematical cell model similarly indicate that an increase in $[\text{Na}]_i$ may indeed shift the timing of NCX forward mode activity during the cardiac cycle leading to reduced forward mode activity during cardiomyocyte relaxation, supporting a role for increased $[\text{Na}]_i$ sensed by NCX in the observed cardiomyocyte phenotype (online supplementary Figure S1C). While $[\text{Na}]_i$ may enhance NCX reverse mode and decrease forward mode, the net effect of the NCX has to be extrusion of external Ca^{2+} entering via the L-type Ca^{2+} channels to maintain a steady state over the whole cardiac cycle.¹⁶ Several sources of excess $[\text{Na}]_i$ may be conceivable: (i) increased NCX activity *per se* may be responsible for increased Na^+ influx and thus $[\text{Na}]_i$, which at a later phase of the cardiac cycle (depending on the transsarcolemmal membrane potential) may then trigger increased reverse-mode activity; (ii) increased Ca^{2+} influx through other channels (e.g. L-type Ca^{2+} or transient receptor potential channels) accumulating Na^+ via forward-mode NCX in NXT animals. Based on our data, however, we consider this unlikely as increased transsarcolemmal Ca^{2+} influx in combination with NCX inhibition with ORM-11035 would aggravate diastolic Ca^{2+} load, which is not what we have observed; (iii) increased Na^+ load through other channels which in the presence of ORM-11035 would no longer be translated into increased $[\text{Ca}^{2+}]_i$. transient receptor potential channels, the late Na^+ current, sodium-proton exchanger and reduced Na^+/K^+ -ATPase (NKA) activity have been described as sources for increased $[\text{Na}]_i$ in remodelled cardiomyocytes. Interestingly, in the present model, protein expression of

the NKA alpha1 and alpha2 isoforms was significantly reduced in NXT² (Figure 5E and 5F).

At the cardiomyocyte level, in HFpEF animals, chronic treatment with ORM-11035 induced alterations in cytosolic Ca^{2+} handling, which are not readily explained by inhibition of NCX alone. This is not unexpected as intracellular Ca^{2+} in cardiomyocytes is highly controlled by feedback mechanisms, and even very specific modulation of one target will affect several regulators of intracellular Ca^{2+} .^{17,18} Indeed, the more rapid diastolic Ca^{2+} removal with ORM-11035 (Figures 4F and 5E) not only improved non-SERCA-dependent Ca^{2+} removal during caffeine application usually attributed to NCX (Figure 5D), but also significantly accelerated the SERCA-related decay of the stimulated Ca^{2+} transient (Figure 5F). The calculated not SERCA-related decay of the stimulated Ca^{2+} transient in NXT + ORM was more variable and not significantly different from NXT. The cause of this additional degree of variation is not clear; however, the difference in the directly measured not SERCA-related decay constant during the caffeine response between NXT and NXT + ORM was highly significant and underscores the altered role of not SERCA-related decay following ORM-11035 treatment. As neither diastolic $[\text{Ca}^{2+}]_i$ nor SR $[\text{Ca}^{2+}]_i$ were affected by chronic ORM-11035, a reduction of Ca^{2+} influx by functional inhibition of the L-type Ca^{2+} channel by sub-sarcolemmal Ca^{2+} may act as compensatory as has been shown in NCX1 knock-out mice.¹⁹ The relevance of ORM-11035 for excess sodium via the NCX and a phase shift in NCX forward-mode activity in HFpEF needs to be explored in future studies.

In summary, specific chronic NCX inhibition triggered adaptation of the highly controlled intracellular Ca^{2+} balance and

cardiomyocyte phenotype that contributed to improved cardiac function *in vivo*.

Irrespective of the origin of ionic dysbalance, we have shown previously that in the present HFpEF model NCX forward-mode activity during diastole is reduced and that the NCX inhibitor SEA0400 improves diastolic Ca^{2+} decay.² NCX inhibition may provide a therapeutic target. This is in line with the beneficial effects of NCX inhibition in other conditions of increased cardiomyocyte Ca^{2+} load such as myocardial ischaemia/reperfusion damage and Ca^{2+} -mediated arrhythmias.^{20,21}

However, within a magnitude of commonly used dosage, SEA0400 also acts on other ion channels, mainly L-type Ca^{2+} channels,^{22,23} and KB-R7943, another commonly used NCX inhibitor, does not allow for higher specificity.²⁴ Recently, several novel orally available NCX inhibitors with significantly higher specificity than SEA0400 have been introduced and proved beneficial to treat experimental arrhythmias.^{20,21} In the present study, ORM-11035, a derivative of ORM-10103, showed a 30-fold higher sensitivity to NCX than L-type Ca^{2+} channels, confirming a much higher specificity for NCX than SEA0400 or KB-R7943 and no apparent effects on cardiac action potential. Systemic blood pressure, which is elevated early as one trigger of cardiac dysfunction and HFpEF in this model, was also not affected. SEA0400 on the other hand has been shown to decrease^{2,25} or increase^{26,27} systemic blood pressure. Blood pressure-lowering effects may also be mediated by (renal) vascular NCX1 in some models of hypertension.²⁵ However, as in the present model with comparable effect on cardiac remodelling SEA0400 reduced blood pressure but ORM-11035 did not, we conclude that this reflects higher specificity of ORM-11035.

We have chosen to study cardiomyocyte function from chronically ORM-11035-treated animals in the absence of ORM-11035 *in vitro*. A limitation is that additional acute effects of therapeutic levels of ORM-11035 on cardiomyocyte function may not be picked up in the *in vitro* experiments. However, this approach allowed us to compare the chronic adaptation of intrinsic cardiomyocyte contractility and Ca^{2+} using identical standardized conditions in all groups. A good *in vitro/in vivo* correlation of diastolic function confirmed that the beneficial effects of ORM-11035 on cardiomyocyte function reflected improved function *in vivo*.

Interestingly, in the present study, chronic NCX inhibition with ORM-11035 also improved maladaptive hypertrophic myocardial remodelling in HFpEF rats *in vivo*. We and others have previously shown that chronically increased diastolic cardiomyocyte Ca^{2+} load can be a trigger of cardiomyocyte hypertrophy.²⁸ Thus, a reduction in cardiomyocyte Ca^{2+} load with ORM-11035 may have contributed to reverse remodelling in HFpEF rats in the present study. In addition, myocardial dysfunction in HFpEF is often associated with increased fibrosis. In the present model as well as in a rat model of hypertensive HFpEF (Dahl salt-sensitive rats) amelioration of HFpEF following NCX inhibition with SEA0400 was associated with reduced myocardial fibrosis.^{2,12} A similar preventive effect of NCX inhibition with SEA0400 was observed when myocardial fibrosis was triggered by increased reverse-mode NCX activity following chronic ouabain treatment in rats,¹²

corroborating a role for reverse-mode NCX in cardiomyocyte dysfunction and increased fibrosis in HFpEF.

Study limitations

As reported here and previously,² the current model reflects many features of clinical HFpEF. However, contribution of NCX to cytosolic Ca^{2+} transients may differ in larger animals and humans. In addition, the efficacy of NCX inhibition may vary in HF of different aetiologies. While published data suggest a stronger role for NCX in larger animals, and predominantly reverse-mode NCX (Ca^{2+} intrusion) has been observed in human HFpEF,¹⁴ the role of NCX inhibition with ORM-11035 in human diseased myocardium needs to be confirmed.

Conclusion

ORM-11035 improves cardiac remodelling and contractile function in a cardiorenal model of HFpEF. Our results indicate that novel, more specific NCX inhibitors do not only provide benefit in Ca^{2+} -mediated arrhythmias as reported earlier but may also provide a promising approach to treat HF. Improvements in cardiac function and remodelling are observed in the absence of blood pressure-lowering effects. Thus, specific NCX inhibitors may provide a therapeutic approach to improve cardiac function and myocardial remodelling in cardiorenal HFpEF patients.

Supplementary Information

Additional supporting information may be found online in the Supporting Information section at the end of the article.

Methods S1. Supplementary methods.

Table S1. Morphometry, renal function and non-invasive blood pressure.

Table S2. Echocardiography, pressure volume and biomarker measurements.

Table S3. Cell shortening amplitude and fluorescence values of Ca^{2+} transients.

Table S4. Ratiometric Ca^{2+} transients.

Figure S1. Simulation of the effects of altered $\text{Na}^+/\text{Ca}^{2+}$ exchanger and SERCA activity on the Ca^{2+} transient.

Figure S2. Chronic treatment with ORM-11035 has no effect on systemic blood pressure in nephrectomy-treated and Sham animals.

Figure S3. ORM-11035 selectivity. Concentration–response curve for human NCX 1.1 reverse-mode Ca^{2+} -influx inhibition by ORM-11035 and L-type Ca^{2+} channel-dependent Ca^{2+} influx inhibition.

Figure S4. Experimental protocol for long-term treatment with ORM-11035 in Sham and nephrectomy-treated rats.

Acknowledgements

We thank Tymon J. Heinzl for his support in data analysis.

Funding

The study was supported by PhD Programme Molecular Medicine of the Medical University of Graz, Austria, and the Ludwig Boltzmann Institute for Translational Heart Failure Research, Graz, Austria.

Conflict of interest: Orion Pharma provided ORM-11035 used for this study. P.P., employed by Orion Pharma, has been involved in the development of ORM-11035. The other authors have nothing to declare.

References

- Senni M, Paulus WJ, Gavazzi A, Fraser AG, Diez J, Solomon SD, Smiseth OA, Guazzi M, Lam CS, Maggioni AP, Tschope C, Metra M, Hummel SL, Edelmann F, Ambrosio G, Stewart Coats AJ, Filippatos GS, Gheorghide M, Anker SD, Levy D, Pfeffer MA, Stough WG, Pieske BM. New strategies for heart failure with preserved ejection fraction: the importance of targeted therapies for heart failure phenotypes. *Eur Heart J* 2014;**35**:2797–2815.
- Primessnig U, Schonleitner P, Holl A, Pfeiffer S, Bracic T, Rau T, Kapl M, Stojakovic T, Glasnov T, Leineweber K, Wakula P, Antoons G, Pieske B, Heinzel FR. Novel pathomechanisms of cardiomyocyte dysfunction in a model of heart failure with preserved ejection fraction. *Eur J Heart Fail* 2016;**18**:987–997.
- Amann K, Neimeier KA, Schwarz U, Törnig J, Matthias S, Orth SR, Mall G, Ritz E. Rats with moderate renal failure show capillary deficit in heart but not skeletal muscle. *Am J Kidney Dis* 1997;**30**:382–388.
- Hohendanner F, Ljubojevic S, Macquaide N, Sacherer M, Sedej S, Biesmans L, Wakula P, Platzer D, Sokolow S, Herchuelz A, Antoons G, Sipido K, Pieske B, Heinzel FR. Intracellular dyssynchrony of diastolic cytosolic $[Ca^{2+}]$ decay in ventricular cardiomyocytes in cardiac remodeling and human heart failure. *Circ Res* 2013;**113**:527–538.
- Sacherer M, Sedej S, Wakula P, Wallner M, Vos M, Kockskamper J, Stiegler P, Sereinigg M, von Lewinski D, Antoons G, Pieske BM, Heinzel FR; CONTICA Investigators. JTV519 (K201) reduces sarcoplasmic reticulum Ca^{2+} leak and improves diastolic function in vitro in murine and human non-failing myocardium. *Br J Pharmacol* 2012;**167**:493–504.
- Mahajan A, Sato D, Shiferaw Y, Baher A, Xie LH, Peralta R, Olcese R, Garfinkel A, Qu Z, Weiss JN. Modifying L-type calcium current kinetics: consequences for cardiac excitation and arrhythmia dynamics. *Biophys J* 2018;**94**:411–423.
- Mahajan A, Shiferaw Y, Sato D, Baher A, Olcese R, Xie LH, Yang MJ, Chen PS, Restrepo JG, Karma A, Garfinkel A, Qu Z, Weiss JN. A rabbit ventricular action potential model replicating cardiac dynamics at rapid heart rates. *Biophys J* 2008;**94**:392–394.
- Fang JC. Heart failure with preserved ejection fraction: a kidney disorder? *Circulation* 2016;**134**:435–437.
- Gori M, Senni M, Gupta DK, Charytan DM, Kraigher-Krainer E, Pieske B, Claggett B, Shah AM, Santos AB, Zile MR, Voors AA, McMurray JJ, Packer M, Bransford T, Lefkowitz M, Solomon SD; PARAMOUNT Investigators. Association between renal function and cardiovascular structure and function in heart failure with preserved ejection fraction. *Eur Heart J* 2014;**35**:3442–3451.
- Ponikowski P, Voors AA, Anker SD, Bueno H, Cleland JG, Coats AJ, Falk V, González-Juanatey JR, Harjola VP, Jankowska EA, Jessup M, Linde C, Nihoyannopoulos P, Parissis JT, Pieske B, Riley JP, Rosano GM, Ruilope LM, Ruschitzka F, Rutten FH, van der Meer P. 2016 ESC Guidelines for the diagnosis and treatment of acute and chronic heart failure: the Task Force for the diagnosis and treatment of acute and chronic heart failure of the European Society of Cardiology (ESC). Developed with the special contribution of the Heart Failure Association (HFA) of the ESC. *Eur J Heart Fail* 2016;**18**:891–975.
- Paulus WJ, Tschope C. A novel paradigm for heart failure with preserved ejection fraction: comorbidities drive myocardial dysfunction and remodeling through coronary microvascular endothelial inflammation. *J Am Coll Cardiol* 2013;**62**:263–271.
- Kamimura D, Ohtani T, Sakata Y, Mano T, Takeda Y, Tamaki S, Omori Y, Tsukamoto Y, Furutani K, Komiya Y, Yoshika M, Takahashi H, Matsuda T, Baba A, Umemura S, Miwa T, Komuro I, Yamamoto K. Ca^{2+} entry mode of Na^{+}/Ca^{2+} exchanger as a new therapeutic target for heart failure with preserved ejection fraction. *Eur Heart J* 2012;**33**:1408–1416.
- Ottolia M, Torres N, Bridge JH, Philipson KD, Goldhaber JJ. Na/Ca exchange and contraction of the heart. *J Mol Cell Cardiol* 2013;**61**:28–33.
- Piacentino V 3rd, Weber CR, Chen X, Weisser-Thomas J, Margulies KB, Bers DM, Houser SR. Cellular basis of abnormal calcium transients of failing human ventricular myocytes. *Circ Res* 2003;**92**:651–658.
- Weber CR, Piacentino V III, Houser SR, Bers DM. Dynamic regulation of sodium/calcium exchange function in human heart failure. *Circulation* 2003;**108**:2224–2229.
- Bridge JH, Smolley JR, Spitzer KW. The relationship between charge movements associated with Ca^{2+} and Na^{+} - Ca^{2+} in cardiac myocytes. *Science* 1990;**248**:376–378.
- Pott C, Yip M, Goldhaber JJ, Philipson KD. Regulation of cardiac L-type Ca^{2+} current in Na^{+} - Ca^{2+} exchanger knockout mice: functional coupling of the Ca^{2+} channel and the Na^{+} - Ca^{2+} exchanger. *Biophys J* 2007;**92**:1431–1437.
- Eisner DA, Caldwell JL, Kistamás K, Trafford AV. Calcium and excitation-contraction coupling in the heart. *Circ Res* 2017;**121**:181–195.
- Reuter H, Henderson SA, Han T, Mottino GA, Frank JS, Ross RS, Goldhaber JJ, Philipson KD. Cardiac excitation-contraction coupling in the absence of Na^{+} - Ca^{2+} exchange. *Cell Calcium* 2003;**34**:19–26.
- Kohajda Z, Farkas-Morvay N, Jost N, Nagy N, Geramipour A, Horvath A, Varga RS, Hornyik T, Corici C, Acsai K, Horváth B, Prorok J, Ördög B, Déri S, Tóth D, Levijoki J, Pollesello P, Koskelainen T, Otsomaa L, Tóth A, Baczkó I, Leprán I, Nánási PP, Papp JG, Varró A, Virág L. The effect of a novel highly selective inhibitor of the sodium/calcium exchanger (NCX) on cardiac arrhythmias in in vitro and in vivo experiments. *PLoS One* 2016;**11**:e0166041.
- Kormos A, Nagy N, Acsai K, Vaczi K, Agoston S, Pollesello P, Levijoki J, Szentandrassy N, Papp JG, Varró A, Tóth A. Efficacy of selective NCX inhibition by ORM-10103 during simulated ischemia/reperfusion. *Eur J Pharmacol* 2014;**740**:539–551.
- Birinyi P, Toth A, Jona I, Acsai K, Almasy J, Nagy N, Prorok J, Gherasim I, Papp Z, Hertelendi Z, Szentandrassy N, Banyasz T, Fulop F, Papp JG, Varró A, Nánási PP, Magyar J. The Na^{+}/Ca^{2+} exchange blocker SEA0400 fails to enhance cytosolic Ca^{2+} transient and contractility in canine ventricular cardiomyocytes. *Cardiovasc Res* 2008;**78**:476–484.
- Tanaka H, Nishimaru K, Aikawa T, Hirayama W, Tanaka Y, Shigenobu K. Effect of SEA0400, a novel inhibitor of sodium-calcium exchanger, on myocardial ionic currents. *Br J Pharmacol* 2002;**135**:1096–1100.
- Hobai IA, O'Rourke B. The potential of Na^{+}/Ca^{2+} exchange blockers in the treatment of cardiac disease. *Expert Opin Investig Drugs* 2004;**13**:653–664.
- Iwamoto T, Kita S, Zhang J, Blaustein MP, Arai Y, Yoshida S, Wakimoto K, Komuro I, Katsuragi T. Salt-sensitive hypertension is triggered by Ca^{2+} entry via Na^{+}/Ca^{2+} exchanger type-1 in vascular smooth muscle. *Nat Med* 2004;**10**:1193–1199.
- Farkas AS, Acsai K, Nagy N, Toth A, Fulop F, Seprenyi G, Birinyi P, Nánási PP, Forster T, Csanády M, Papp JG, Varró A, Farkas A. Na^{+}/Ca^{2+} exchanger inhibition exerts a positive inotropic effect in the rat heart, but fails to influence the contractility of the rabbit heart. *Br J Pharmacol* 2008;**154**:93–104.
- Yatabe MS, Yatabe J, Takano K, Sanada H, Kimura J, & Watanabe T. Effects of renal Na^{+}/Ca^{2+} exchanger 1 inhibitor (SEA0400) treatment on electrolytes, renal function and hemodynamics in rats. *Clin Exp Nephrol* 2015;**19**:585–590.
- Sedej S, Schmidt A, Denegri M, Walther S, Matovina M, Arnstein G, Gutsch EM, Windhager I, Ljubojevic S, Negri S, Heinzel FR, Bisping E, Vos MA, Napolitano C, Priori SG, Kockskamper J, Pieske B. Subclinical abnormalities in sarcoplasmic reticulum Ca^{2+} release promote eccentric myocardial remodeling and pump failure death in response to pressure overload. *J Am Coll Cardiol* 2014;**63**:1569–1579.